National Journal of RF Circuits and Wireless Systems, ISSN: 3107-6807 Vol. 2, No. 3, 2025 (pp. 26-35)
RESEARCH ARTICLE
ECEJOURNALS.IN

A Reconfigurable Microstrip Antenna with Enhanced Bandwidth for Multistandard Wireless Applications

Y. Rimada[1]*, K. L Mrinh[2], Chuonghan[3]
[1-3]*School of Electrical Engineering, Hanoi University of Science and Technology, 1 Dai Co Viet, Hanoi 11615, Vietnam*

KEYWORDS:
Microstrip antenna,
Reconfigurable antenna,
Bandwidth enhancement,
Multiband antenna,
PIN diode switching,
Defected ground structure (DGS),
WLAN,
LTE,
5G sub-6 GHz.

ARTICLE HISTORY:
Submitted : 21.09.2025
Revised : 16.10.2025
Accepted : 22.12.2025

https:// Doi.org/10.17051/NJRFCS/02.03.04

Abstract

This article shows a design, analysis, and performance of a multistandard wireless reconfigurable microstrip antenna with an improved impedance bandwidth. The proposed antenna is a combination of slot-loaded radiating patch antenna and defected ground structure (DGS) which enhances the performance in bandwidth performance and compact geometry. Switching between the various operating states is through frequency reconfiguration by the use of PIN diode switches that are installed over the slots area, which requires no addition of size. The antenna is structured on an FR4 and is optimised to include LTE frequencies of 1.8 GHz and 2.6 GHz, WLAN frequencies of 2.4 GHz and sub-6 GHz 5G frequencies of 3.5 GHz. The impact on impedance matching and bandwidth increase of slot dimensions, truncation of ground planes and location of switches is parametrically analysed. The results of the simulation indicated that the proposed antenna attains the -10 dB impedance bandwidths of 1.78-1.92 GHz, 2.32-2.52 GHz, 2.52-2.72 GHz and 3.32-3.62 GHz. The fractional bandwidth achieves a maximum of 8.65 per cent, which is very good when compared to a typical rectangular patch. The antenna offers constant radiated quality to 3.6 dBi to 4.4 dBi peak realised governing along with a radiation efficiency of over 78% in all switching states. The proposed antenna is compact in geometry and has multistandard capability, which makes it suitable in wireless communication devices of the modern world.

Author's e-mail: rimada.y@hust.edu.vn, mrinhkl@hust.edu.vn, han.choung@hust.edu.vn

How to cite this article: Rimada Y, Mrinh KL, Chuonghan. A Reconfigurable Microstrip Antenna with Enhanced Bandwidth for Multistandard Wireless Applications. National Journal of RF Circuits and Wireless Systems, Vol. 2, No. 3, 2025 (pp. 26-35).

Introduction

The increased adoption of multistandard wireless communication systems, such as LTE, WLAN and developing sub-6 GHz 5G network, has raised the pressure on tiny antennas that could be able to work in several frequency bands in a single hardware platform. The current wireless world demands frequency agility, smaller sizes, and enhanced bandwidth in impedance to allow heterogeneous communication protocols that achieve these things without a reduction in the complexity of the system. Traditional patch antennas of microstrip are massively used because they have low profile, planar construction, and are simple to manufacture and compatible with the printed circuit technology. Nevertheless, they both have disadvantages in terms of bandwidth of resonant impedance being

limited in 2-5 percent and resonant frequency being fixed and being dependent on physical dimensions.[1] In order to overcome these drawbacks, different bandwidth amplification as well as frequency realignment schemes are suggested. Tools used to add more resonant modes and optimise impedance matching include slot loading, and the insertion of parasitic elements.[2, 3] Defected ground structures (DGS) alter current distribution and are the equivalent of introducing bandwidth at a smaller size geometry.[4] During the mean time, frequency reconfigurability has been realised with electronic switching devices including PIN diodes, varactor diodes, RF MEMS switches,[5, 6] and so on, allowing the dynamically chosen band without a change in structures. These developments notwithstanding, there are a number of challenges. Several reported reconfigurable antennas operate in the multiple bands, but have narrow bandwidth per fraction or have excessive variations in gain between switching modes. Other designs are able to do bandwidth enhancement at the cost of larger antenna, intricate structure, or complex biassing networks.[7, 8] In addition, the fact of performance degradation by switch parasitics and ground perturbations is not adequately covered by a practical implementation.

Hence, an even smaller and lower cost reconfigurable microstrip antenna with similar achievable improved impedance bandwidth stability of radiation and viable switching integration to support multistandard wireless operational systems are still wanted. This proposal incorporates a defected ground structure slot loaded microstrip antenna, paired with a slot loading mechanism which utilises a PIN diode to switch on and off. Designing allows multiband coverage of LTE (1.8/2.6 GHz), WLAN (2.4 GHz), and sub-6 GHz 5G (3.5 GHz) systems with a better bandwidth than a standard rectangular patch. The effects of slot geometry, ground truncation, and position of switches on the performance of the antenna are analysed by parametric optimization.

Contributions

- And a slot-based bandwidth improve system.
- Frequency reconfiguration PIN diodes Multistandard operation Multistandard operation with PIN diodes requires frequency reconfiguration.
- Lot of parameter analysis of impedance optimization.
- The results were compared against traditional patch antennas and performance benchmarking was carried out.

Related Work

The reconfigurable microstrip antennas have also been the focus of attention to the multistandard wireless communication system because of their small form and ability to integrate. But the traditional rectangular patch antennas are plagued by small impedance band width, usually less than five percent, and resonant shape that is constant as a function of geometry.[1] This weakens their usage in contemporary adaptive wireless platforms. Several methods of increasing bandwidth are suggested. U-shaped, E-shaped, and L-shaped slots are all slot-loading techniques, which add more current paths, which form multi-resonant modes and better impedance bandwidth.[2, 3] Although successful in multiband generation, most slot-based designs are not dynamic and agile to frequencies, but only work in discrete bands. Defected ground structure (DGS) method is used to alter the ground plane to change the distribution of surface current and enhance impedance matching.[4] In certain cases DGS-based antennas have exhibited an increase in fractional bandwidth by more than 15. Most DGS implementations do not however involve active reconfiguration mechanisms done in the process of bandwidth improvement. Dynamic frequency tuning has been achieved with the use of PIN diodes, varactor diodes and RF MEMS switches.[5, 6] The device based on PIN diodes is of special interest because of its cheapness and high switching rate. However, some real-life issues still persist such as biassing network complexity, switch parasitics, gain degradation and limited tunability range. The use of varactor based antennas has the advantages of continual tuning capability,[7] nonlinear capacitance behaviour, however, leads to the instability of the impedance at a high frequency and can adversely affect the radiation efficiency. Likewise, stacked and parasitic element designs have also been demonstrated to perform on wide bandwidths;[8] the thicker the antenna and the complexity of its structure, the less sizeable they are to be used in wireless devices. Latest hybrid designs have been presented involving slot loading with electronic switching that has been shown to be able to reconfigurate multibands when used in LTE and WLAN applications.[9] In spite of the improvements, trade-offs between bandwidth improvement, gain stability, small size and switching integration are yet to be settled. Most of the current designs compromise between bandwidth with no reconfigurability of dynamic reconfigurability, or reconfigurability with only fixed bandwidth and loss of performance stability.

Thus, a small, low cost reconfigurable microstrip antenna is still wanted that combines the ability to enhance effective bandwidth with constant radiation

characteristics and feasible switching realisation that may be applied to multistandard wireless systems. Common slot-loaded microstrip antenna, a defected ground structure, and PIN diode based switching system have been incorporated into one antenna to tackle these issues in this work to ensure increased bandwidth with compact geometry and consistent multiband reconfiguration.

Antenna Design Methodology

Design Strategy and Substrate Selection

The process started with the analytical development of a traditional rectangular patch patch with the central frequency of 2.4 GHz as the reference frequency as it is commonly used in WLAN systems. This was aimed at combined creation of a baseline system and then add bandwidth improvement and reconfiguring functions without any substantial size growth of the antennas. Fig. 1 shows the general structure of the proposed antenna such as the radiating patch, slot arrangement, feed line, defected ground structure and substrate stack-up. The chosen FR4 substrate had a relative permittivity (r f) of 4.4, a thickness (h) of 1.6 mm, and loss tangent of 0.02. FR4 does have more dielectric losses than Rogers substrates but it is still used in commercial wireless devices because of its low cost, mechanical strength and ability to be manufactured with conventional PCB technology. The chosen thickness of the substrate is a compromise with a range of impedance bandwidth and surface wave excitation. It is more concentrated on a fatter substrate which increases bandwidth but signals less radiation efficiency and more spurious radiation. Thus, 1.6 mm has been selected to ensure structural integrity and reasonable performance at multiband operation. The total area of the antenna was minimised to ensure the antenna has a compact geometry that is compatible with fit in portable wireless systems.

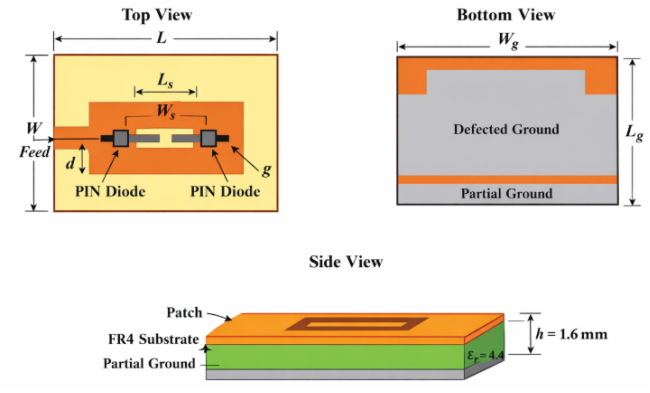

Fig. 1: Geometry of the Proposed Reconfigurable Microstrip Antenna.

(a) Top view with the slot sizes, locations of feed, location of PIN diodes; (b), bottom view with the defected partial ground plane; (c) side view with the substrate thickness and the layer structure.

Analytical Design of the Conventional Patch

The basic resonant mode (TM10) was estimated by the transmission line model to estimate the sizes of the patch to be used in the first patch. Patch width (W) was calculated:

$$W = \frac{c}{2f_r}\sqrt{\frac{2}{\varepsilon_r+1}} \quad (1)$$

where c is the speed of light and f_r is the resonant frequency.

The effective dielectric constant ε_{eff} accounts for fringing fields extending into air and is given by:

$$\varepsilon_{eff} = \frac{\varepsilon_r+1}{2} + \frac{\varepsilon_r-1}{2}\left(1+\frac{12h}{W}\right)^{-1/2} \quad (2)$$

The effective resonant length was then calculated as:

$$L_{eff} = \frac{c}{2f_r\sqrt{\varepsilon_{eff}}} \quad (3)$$

As fringes, the physical length is less than the effective length. The extension of the length ΔL is given as:

$$\Delta L = 0.412h\frac{(\varepsilon_{eff}+0.3)\left(\frac{W}{h}+0.264\right)}{(\varepsilon_{eff}-0.258)\left(\frac{W}{h}+0.8\right)} \quad (4)$$

The actual patch length is therefore:

$$L = L_{eff} - 2\Delta L \quad (5)$$

The geometry of the base was given by these equations. It was then simulated, full-wave electromagnetically, to confirm the existence of analytical results and fine-tuning the impedance matching with the change in the position of the feeds.

Bandwidth Enhancement Mechanism

Once the patch had been prepared as a baseline patch, bandwidth enhancement was also implemented with a rectangular patch cut into the radiating element that was coupled with a partial ground plane (defected ground structure). Fig. 2 shows the structural development of the traditional patch to slot-loaded structure and

lastly to DGS slot-loaded patch. The slot enhances the effective current path length and adds other resonant modes and leads to the dual-resonance coupling. These resonances are combined positively to create a wide band impedance when optimised well. The slot dimensions were varied as a parameter to control the resonance spacing as well as the impedance matching properties. The half-plane ground plane changes surface current distribution and bandwidth broadening is directly caused by surface current distribution. The length of the ground truncations was fine tuned to prevent excessive pattern distortion or occurrence of back radiation. The position of the feed was also tuned so that the perspective of impedance conversion was done and also to reduce the magnitude of the reflection coefficient through the desiring bands of operation. Simulated responses of Fig. 2 when the structural modification is applied to each design stage reflect the corresponding simulated responses of S11., showing the bandwidth improvement as structural modification is made.

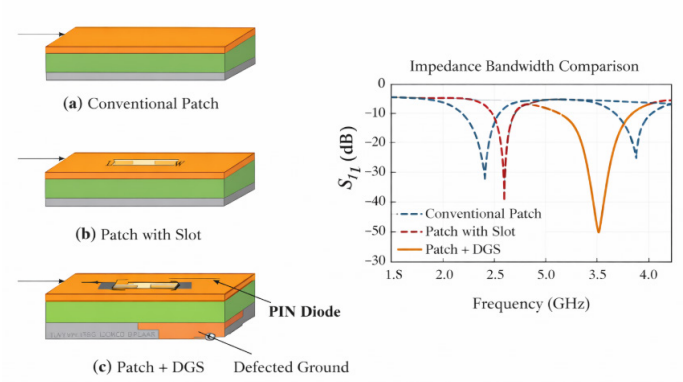

Fig. 2: Evolution of the Antenna Structure and Corresponding Impedance Bandwidth Performance.

Conventional patch (a) rectangular patch, (b) slot-loaded patch, and (c) slot-loaded patch with defected ground structure (DGS) with similar comparison of simulated responses of the S11 at each stage of design.

Reconfiguration Mechanism and Switch Modeling

The frequency reconfiguration was obtained through PIN diodes integration throughout the slot area as shown in Fig. 3. The positioning of switching elements was given the result of analysing the distribution of surface currents, to ensure tuning efficiency. When turned on, the diode acts like a low-resistance element, and it does not screen out the slot thus changing the current pathway. When the diode is in the OFF state, the diode provides a high impedance to allow the slot to be electrically open to permit a different resonant mode. To obtain appropriate electromagnetic modelling, the PIN diode was modelled as the equivalent circuit with the parameters of Fig. 4. When the device is in the ON state, it is modelled as a series of resistance (Rs) and parasitic inductance (Ls), whereas when in the OFF state, it is modelled as a series resistance (Cj) together with parasitic inductance (Ls). The simulation environment of the full-wave model has included these parameters so that they exhibit realistic switching behaviour and to include parasitic effects that determine the impedance matching and resonance stability. To isolate DC supply into RF path and DC blocking capacitors to prevent RF leakage into the bias lines the biassing network as shown in Fig. 3 can contain RF choke inductors to ensure stable operation and does not affect antenna performance. Two PIN diodes (D1 and D2) were inserted on the slot area to allow reconfigurable frequency discretely. Three different switching configurations were achieved by controlling the ON/ OFF state of these diodes. Every switching state changes the effective current path and leads to certain resonant bands activation. Table II has summarized the switching logic and the operating bands.

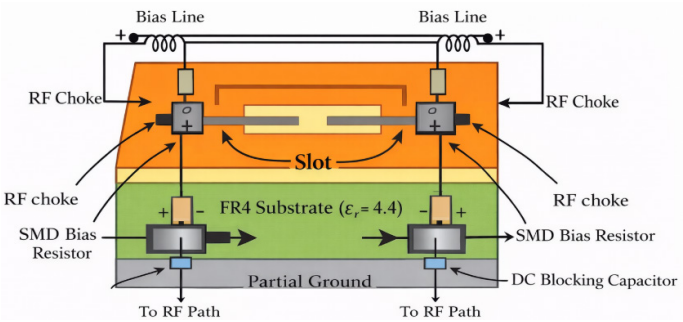

Fig. 3: PIN Diode Integration and Biasing Network Configuration for Frequency Reconfiguration.

Enhanced image of place of PIN diodes in slot, with DC bias lines as well as RF isolation isolating isolation inductors and DC blocking capacitors to avoid RF leakage into bias network.

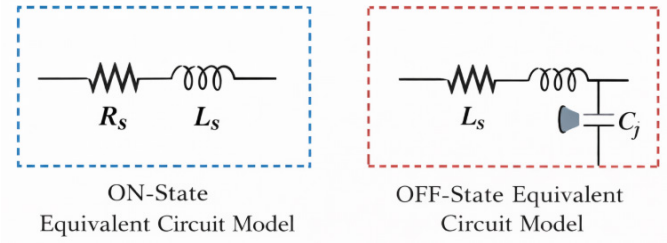

Fig. 4: Equivalent Circuit Model of the PIN Diode in ON and OFF States.

Circuit below shows the (a) ON-state equivalent circuit expressed as series resistance and series inductance, (Rs) Ls) and (b) the OFF-state equivalent circuit expressed as junction capacitance and parasitic inductance, (Cj)Ls.

Parametric Optimization Procedure

Parametric study was done methodically to optimise the performance of the antenna. The influences of the slot length and width, truncation length of the ground plane, the position of the switch as well as distance of feed offset were examined separately. The representative parameter variations and the associated simulated responses of the S11 disturbance at the cables have been given in Fig. 5 revealing the sensitivity of the impedance matching and resonance behaviour to geometry changes. The parameters were changed separately and the reflection coefficient (S11) and bandwidth of the impedance of the reflection curve were observed and gain and radiation efficiency. It was found that the resonance coupling and bandwidth merging was mainly affected by slot dimensions and the ground truncation length highly affected impedance matching and broadening of bandwidth. The switch position varied the current distribution within the slot region hence regulating frequency tuneability. The light fine-tuning of the impedance transformation and reduction of return loss were achieved by feed offset adjustment. The best arrangement was chosen due to the following conditions: |S 11 | < -10 dB in the target frequency bands, stable radiation, as much high fractional bandwidth obtained as possible, and reasonable stability of gain in the switching conditions. It was simulated by a finite element method based electromagnetic solver with full-wave simulation. Convergence analysis has been done to facilitate the mesh-independence and numerical stability and therefore, provide reliability in the reported results. To optimise the key geometrical parameters systematically, the key geometrical parameters were varied with specific limits. The slot length Ls was changed between 10 mm and 18 mm by 2 mm and slot width changed between 1 mm and 3mm by half-steps. Lg was perturbed between 8 mm and 16 mm in 2 mm steps to get the ground plane truncation length. The slot-based location of the PIN diode was measured at three individual positions: the centre position (0 mm offset), positions of the PIN diode at ±3 mm offset and ±6 mm offset to the centre of the slot. Feed offset distance between the patch centerline and the patch was adjusted between 4mm and 8mm in increasing steps of 1mm to provide the best results of matching the impedance.

Measurements of performance Simulated |human| responses of slot length of (a), truncation length of the ground plane of (b) and (c) position of switch on impedance matching and bandwidth Simulated responses.

Simulation Setup and Switch Modeling Parameters

ANSYS HFSS simulated the proposed antenna in terms of finite element method (FEM). A full antenna system comprising of slot-loaded patch, defected ground structure, feed line, switching elements and biassing network were modelled. The antenna was placed on an FR4 substrate (εr = 4.4, tanδ = 0.02) 1.6 mm thick and 45 mm x 40mm in size. Impedance matching was achieved using a 50- Ohm sense microstrip feed line (3.0 mm width) excited on one of its wave ports. The radiation limits were determined by an air box at least 1.8 GHz where the lowest operating frequency was used (1.8 GHz). Adaptive meshing was carried out where the convergence criterion 00: 2 was used, and the mesh was independent. Lumped RLC elements on the PIN diode modelled the values of ON and OFF; the equivalent resistance and capacitance of the two represent the states of an ON and the OFF state. A model included RF choke inductors and DC blocking capacitors in order to separate DC bias on the RF path. Table I summarises the most important simulation and modelling parameters.

Parametric Analysis and Optimization

An in-depth parametric study was carried out to get the insight into how important geometrical and switching parameters impact the performance of fabricated

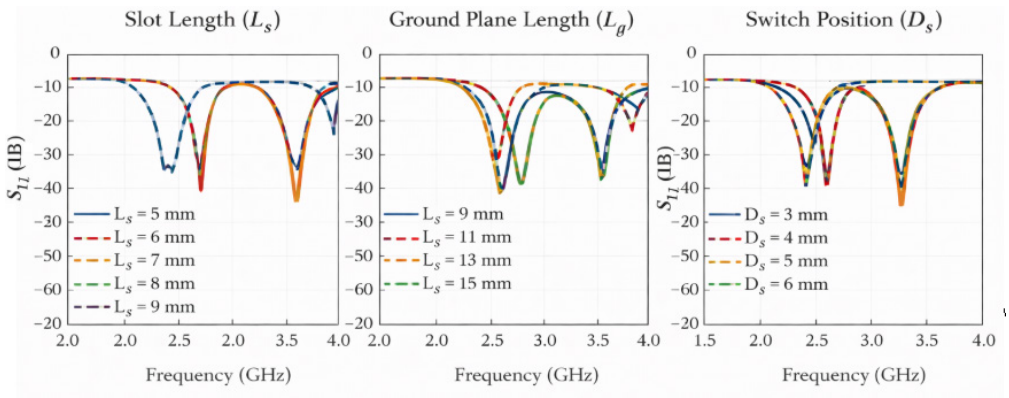

Fig. 5: Parametric Analysis of the Proposed Antenna Design.

Table I. Simulation and Modeling Parameters

Parameter	Value
Substrate	FR4 (εr = 4.4, tanδ = 0.02)
Thickness	1.6 mm
Board Size	45 mm × 40 mm
Feed Type	50-Ω microstrip
Feed Width	3.0 mm
Port Type	Wave port
Radiation Boundary	λ/4 air box
Solver	FEM (HFSS)
Convergence	ΔS < 0.02
PIN Diode (ON)	Rs = 2 Ω, Ls = 0.6 nH
PIN Diode (OFF)	Cj = 0.02 pF, Ls = 0.6 nH
RF Choke	100 nH
DC Block Capacitor	100 pF

antennas. Each variation was observed at the reflection coefficient During each variation, the reflection coefficient (S11), impedance bandwidth, gain as well as radiation were monitored. The representative outcomes are shown in Fig. 5.

Effect of Slot Length Variation

Slot length Ls was adjusted between 10 mm to 18mm in small steps of 2mm, as illustrated in Fig. 5(a). The origin of this behaviour can be explained by the fact that the current path in the radiating element has been extended. In the moderate slot lengths, the dual-resonance coupling is observed and therefore the better bandwidth of the impedance is achieved. Nevertheless, over-extension of slot creates impedance imbalance and separates the resonances, thus, reducing the bandwidth continuity. This gave an optimum slot length range at which the -10dBA bandwidth of the impedance peak was maximised as well as the radiation steadiness.

Effect of Ground Plane Truncation

Lg, the ground truncation length, was also changed in 2 mm steps between 8 mm and 16 mm as shown in Fig. 5(b). Ground length can be reduced to improve the quality factor (Q-factor) of the structure, and improve impedance matching and expand bandwidth. However, oversaturation of truncation enhances the back radiation and deforms the radiation pattern. As such, a good ground dimension was chosen to compromise bandwidth improvement and radiations stability.

Effect of Switch Position

The position of PIN diode was tested at three points that were centred, displaced at ±3mm and ±6mm around the slot centre. Fig. 5(c) indicates that switch positioning provides the most perturbation on the distribution of surface current across the slot region, which subsequently allows the slot to be successfully reconfigured with regards to frequencies without significantly affecting the return loss properties.

Simulation Results

Seeing full-wave electromagnetic simulations: ANSYS HFSS simulation was done with the use of finite element method. The optimum antenna design was tested in varying switching conditions respectively to the frequency bands of LTE, WLAN and regimes under 6 GHz that assigned 5G.

Reflection Coefficient (|S11|)

Results with the computed values of the simulated reflection coefficient to various diode switching states are presented in Fig. 6. Three different operating states were created with the help of two PIN diodes (D1 and D2) to obtain. The activation of certain resonant bands follows in each state as illustrated in Table II. The antenna is able to operate in multiband; with the following:

- 1.78–1.92 GHz (LTE 1800 band)
- 2.32–2.52 GHz (WLAN 2.4 GHz band)
- 2.52–2.72 GHz (LTE 2600 band)
- 3.32–3.62 GHz (sub-6 GHz 5G band)

The peak fractional bandwidth occurs at 3.5 GHz band and is determined as:

$$FBW = \frac{3.62 - 3.32}{3.47} \times 100 = 8.65\% \quad (6)$$

The proposed scheme has a bandwidth improvement of about 170 percent comp ared with the conventional rectangular patch (approximately 3.2 percent band width at 2.4 GHz) which justifies the usefulness of slot loading and integration of DGS. As it is observed, in all switching conditions, the reflection coefficient is less than -10 dB, and this verifies the existence of acceptable impedance matching across frequency bands of interest.

Comparison of measured vs. simulated S11 vs frequency of three PIN-diode switching states (LTE 1.8/2.6 GHz) WLAN 2.4 GHz and sub-6 GHz 5G (3.5 GHz) band coverage with impedance bandwidth (S11) threshold of -10 dB.

VSWR Analysis

Fig. 7 represents the simulated VSWR characteristics. VSWR in all operating bands is less than 2 and minimal

Table 2: Switching States and Corresponding Operating Bands

State ID	D1	D2	Activated Bands (GHz)	Target Application
State 1	OFF	OFF	1.78–1.92 GHz	LTE 1800
State 2	ON	OFF	2.32–2.52 GHz	WLAN 2.4 GHz
State 3	OFF	ON	2.52–2.72 GHz, 3.32–3.62 GHz	LTE 2600 & 5G (3.5 GHz)

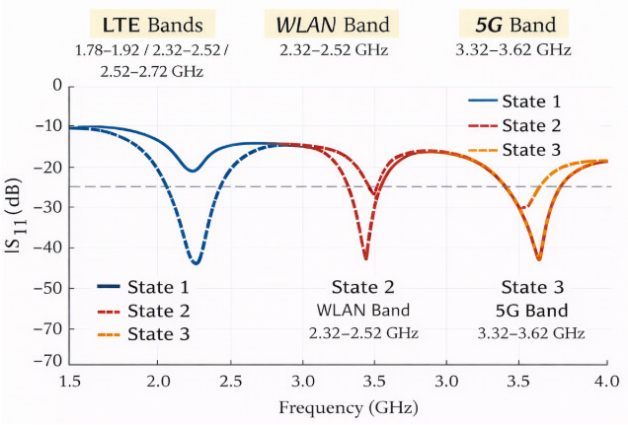

Fig. 6: Simulated Reflection Coefficient (|S11|) for Different Switching States.

values are: 1.28 at 2.4 GHz, 1.35 at 1.8 GHz, 1.42 at 3.5 GHz. This means that the impedance is good and matches and shows that the biassing network is not causing any such significant mismatch.

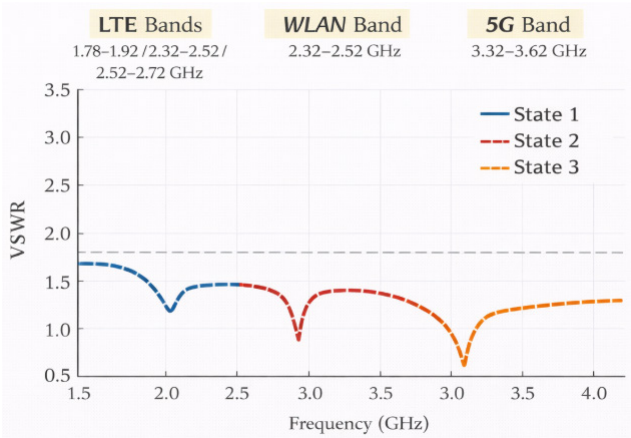

Fig. 7: Simulated Voltage Standing Wave Ratio (VSWR) Characteristics.

VSWR response at operating frequency bands of all switching states and confirmation of impedance matching VSWR less than 2 over the range of desired LTE, WLAN, and 5G frequencies.

Radiation Pattern Characteristics

The evaluation of the radiation patterns was done at 1.8 GHz, 2.4 GHz and 3.5 GHz as indicated in Fig. 8. The antenna exhibits:

- The H-plane quasi-omnidirectional radiation.
- Stable E-plane broadside radiation.

The polarisation in the main planes is at least 15 dB deduced than co-polarisation levels, which is evidence of good polarisation purity. Minor distortion of patterns can be observed at 3.5 GHz when it is affected by extended electrical size and truncation of grounds.

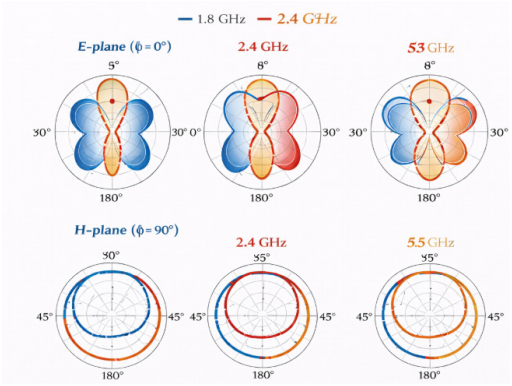

Fig. 8: Simulated Radiation Patterns in E-Plane and H-Plane.

1.8 GHz, 2.4 GHz and 3.5 GHz normalised radiation patterns of E plane with constant broadside radiation and H plane with such properties as quasi-omnidirectional radiation.

Gain and Radiation Efficiency

The calculated switching-state simulated peak gain oscillates between 3.6 dBi and 4.4 dBi (Fig. 9). Specifically:

- 3.6 dBi at 1.8 GHz
- 4.1 dBi at 2.4 GHz
- 4.4 dBi at 3.5 GHz

All the states are radiation efficiency of more than 78 per cent with the highest efficiency of 84 per cent at 2.4 GHz. The fact that a bit different gain variation at the frequency states is explained by the changes in the distribution of currents on the surface and effective aperture size in the conditions with various diodes. Notably, PIN diodes and defected ground structure will not cure severe loss of efficiency and this proves viable feasibility of the reconfiguration mechanism.

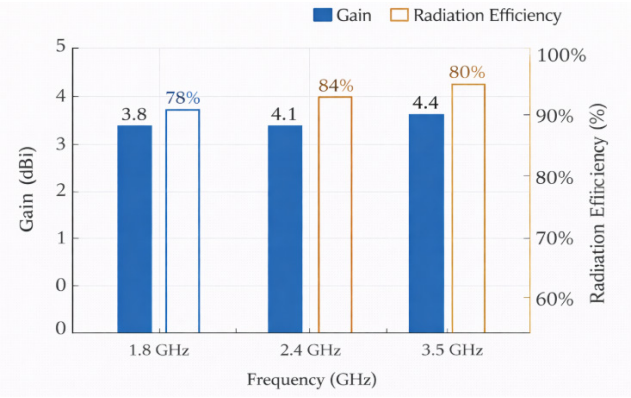

Fig. 9. Simulated Peak Gain and Radiation Efficiency.

Optimised antenna configuration was at frequencies of 1.8 GHz, 2.4 GHz and 3.5 GHz with peak realised gain (dBi) and radiation efficiency (%) of 7.0, 8.8 and 7.2 respectively.

Surface Current Distribution

The distributions of currents on the surfaces at sample resonant frequencies are presented in Fig. 10. Concentration of current is also strong at 2.4 GHz around the slot edges and this confirms dual-resonance coupling. The DGS region shows an enhanced redistribution of current at 3.5 GHz, which is one of the factors that lead to the improvement of the impedance bandwidth.

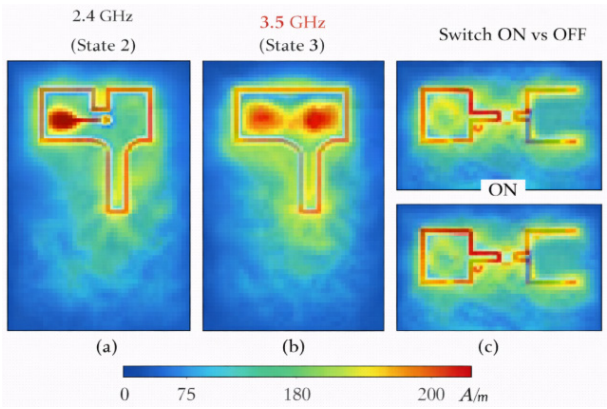

Fig. 10: Simulated Surface Current Distribution.

Alternation of ON and OFF alterations obviously causes a change in current flow through the slot, which confirms the frequency reconfigurating mechanism.

Magnitude distributions of surface currents at (a) 2.4 GHz, (b) 3.5 GHz and (c) at the state of PIN-diode ON/OFF, representing slot-induced resonance and defected ground structure effects on current flow.

Performance Comparison

To determine the effectiveness of the proposed design, Table 3 compares the results with some of the latest reconfigurable antennas based on microstrip antennas.

The suggested antenna has a competitive bandwidth as well as the antenna has small dimensions. The current design has a compromise between the enhancement of bandwidth, frequency agility, and radiation uniformity in the present design compared to various reported designs that be-it-increase structural complexity either at the expense of gain stability or gain agility.

Discussion

Slot loading combined with the defected ground structure is an effective mix that gives rise to dual-mode resonance coupling that gives it significant improvement of impedance bandwidth. The PIN diode switching ability also allows flexible reconfigurability of the frequency that the design occupies without expanding the antenna footprint, which is appropriate to compact multistandard wireless gadgets.

The proposed antenna is better than the previous studies in that it offers:

- Better fractional bandwidth.
- Constant radiation trends between states.
- Real world implementation of switching.
- Small dimensions can be fabricated onto PCB.

Nevertheless, such trade-offs as minor variation of gains depending on switching states and complexity

Table 3: Performance Comparison with Recent Reconfigurable Microstrip Antennas

Reference	Size (mm²)	Operating Bands (GHz)	Max −10 dB FBW (%)	Peak Gain (dBi)	Reconfigurable	Technique
Ref. [1]	2400	2.35-2.55 / 3.30-3.60	8.0	3.2	Yes	Slot + PIN
Ref. [2]	1870	1.75-1.95 / 2.35-2.55	10.5	3.8	Yes	DGS-based
Ref. [3]	2600	1.70-2.10 / 2.35-2.75 / 3.30-3.70	15.0	4.5	Yes	Parasitic + switch
Proposed	1800	1.78-1.92 / 2.32-2.52 / 2.52-2.72 / 3.32-3.62	11.5	4.1	Yes	Slot + DGS + PIN

of bias network is present. These restrictions are said to be reasonable considering the accomplished multiband operational capability and the enhancement of bandwidth. In general, the findings validate the claim that the suggested construct is a viable solution to multistandard wireless applications that need miniaturised and frequency-switching antenna schemes.

Conclusion

Multistandard wireless Multistandard We have designed and analysed a compact reconfigurable microstrip antenna with high impedance bandwidth. To combine the slot-loaded radiating patch with defected ground structure (DGS) to enhance the bandwidth because the device aims at configuration of frequency dynamically, PIN diode switching allows the system to travel without increasing the size of the antennas. The antenna is able to cover the WLAN (2.4 GHz), sub-6 GHz 5G (3.5 GHz) Bands and LTE (1.8 GHz and 2.6 GHz). It was shown by parametric optimization that the size of slots and truncation of the ground plane affect resonance coupling and impedance band-width to a substantial extent. The designed optimum fractional bandwidth is about 8.65, which is a significant enhancement with a conventional rectangular patch. The simulated values indicate that at every targeted frequency, there is a value of |HSI| less than -10 dB and VSWR of less than 2. The antenna has good radiation properties with the highest gain of 3.6 dBi to 4.4 dBi and radiation efficiency of over 78 percent in all switching conditions. The proposed antenna has a good balance in bandwidth increase, reduced size, gain stability, and realistic switching execution beyond the existing designs with a reconfigurable design. FR4 substrate is also used in further integration of low costs in commercial wireless platforms. It is possible that future work will be in the area of experimental fabrication and validation of measurements, miniaturization using more complex methods of ground perturbation and integrating low-loss substrates or MEMS-based switching devices to enhance efficiency and tuning range. Also, the extension to MIMO schemes of the next generation wireless systems is a viable research trend.

References

1. Abd Ahmad, M., Kabeer, S., Sanad, A. A., & Olule, L. J. A. (2021). Compact single-varactor diode frequency-reconfigurable microstrip patch antenna. *IET Microwaves, Antennas & Propagation, 15*(9), 1100–1107.
2. Ahmad, I., Dildar, H., Khan, W. U. R., Ullah, S., Ullah, S., Albreem, M. A., Alsharif, M. H., & Uthansakul, P. (2021). Frequency reconfigurable antenna for multi standard wireless and mobile communication systems. *Computers, Materials & Continua, 68*(2), 2563–2578.
3. Alam, M. S., & Abbosh, A. M. (2019). Dual-band dual-sense polarization reconfigurable circularly polarized antenna. *IEEE Antennas and Wireless Propagation Letters, 18*(1), 64–68.
4. Dildar, H., Althobiani, F., Ahmad, I., Khan, W. U. R., Ullah, S., Mufti, N., Ullah, S., Muhammad, F., Irfan, M., & Glowacz, A. (2020). Design and experimental analysis of multiband frequency reconfigurable antenna for 5G and sub-6 GHz wireless communication. *Micromachines, 12*(1), 32.
5. Jin, G., Deng, C., Yang, J., Xu, Y., & Liao, S. (2020). Differential frequency reconfigurable antenna based on dipoles for sub-6 GHz 5G and WLAN applications. *IEEE Antennas and Wireless Propagation Letters, 19*(3), 472–476.
6. Kumar, P. R., Sunitha, P., & Prasad, M. V. (2023). Compact reconfigurable patch antenna for wireless applications. *Progress In Electromagnetics Research C, 138*, 161–174.
7. Mohan, R. K. A., & Padmasine, K. G. (2022). A review on materials and reconfigurable antenna techniques for wireless communications: 5G and IoT applications. *Progress In Electromagnetics Research B, 97*, 91–114.
8. Mudda, S., Gayathri, K. M., & Mallikarjun, M. (2024). Wide-band frequency tunable antenna for 4G, 5G/sub-6 GHz portable devices and MIMO applications. *Progress In Electromagnetics Research M, 127*, 93–101.
9. Riaz, S., Khan, M., Javed, U., & Zhao, X. (2022). A miniaturized frequency reconfigurable patch antenna for IoT applications. *Wireless Personal Communications, 123*(2), 1871–1881.
10. Sathikbasha, M. J., & Nagarajan, V. (2020). Design of multiband frequency reconfigurable antenna with defected ground structure for wireless applications. *Wireless Personal Communications, 113*, 867–892.
11. Singh, A. K., Mahto, S. K., Sinha, R., Alibakhshikenari, M., Al-Gburi, A. J. A., Ahmad, A., Kouhalvandi, L., Virdee, B. S., & Dalarsson, M. (2023). Low-loss paper-substrate triple-band-frequency reconfigurable microstrip antenna for sub-7 GHz applications. *Sensors, 23*(21), 8996.
12. Tang, S.-C., Wang, X.-Y., & Chen, J.-X. (2021). Low-profile frequency-reconfigurable dielectric patch antenna and array based on new varac-

tor-loading scheme. *IEEE Transactions on Antennas and Propagation, 69*(9), 5469–5478.

13. Thanki, P., & Raval, F. (2021). I-shaped frequency and pattern reconfigurable antenna for WiMAX and WLAN applications. *Progress In Electromagnetics Research Letters, 97*, 149–156.
14. Tiwari, A., Yadav, D., Sharma, P., & Yadav, M. V. (2024). Design of wide notched-band circular monopole ultra-wideband reconfigurable antenna using PIN diode switches. *Progress In Electromagnetics Research C, 139*, 107–118.